[1.]Fatai O. ARAMIDE, [1.]Idris B. AKINTUNDE, [2.]Patricia A. POPOOLA

EFFECTS OF TITANIA-SILICON CARBIDE ADDITIVES ON THE PHASE DEVELOPMENT AND PROPERTIES OF SINTERED MULLITE-CARBON COMPOSITE

[1.]Department of Metallurgical and Materials Engineering,
Federal University of Technology, Akure, NIGERIA
[2.]Department of Chemical, Metallurgical and Materials Engineering,
Tshwane University of Technology, Pretoria West, SOUTH AFRICA

Abstract: The effects of the additives (silicon carbide and titania) and sintering temperatures on the phases developed, physical and mechanical properties of sintered mullite-carbon ceramic composite produced from kaolin and graphite was investigated. The kaolin and graphite of known mineralogical composition were thoroughly blended with 5 and 3 (vol.) % silicon carbide and titania respectively. From the homogeneous mixture of kaolin, graphite and titania, standard samples were prepared via uniaxial compaction. The test samples produced were subjected to firing (sintering) at 1300°C, 1400°C and 1500°C. The sintered samples were characterized for the developed phases using x-ray diffractometry analysis, microstructural morphology using ultra-high resolution field emission scanning electron microscope (UHRFEGSEM). Various physical and mechanical properties were determined. It was observed that the addition of SiC/TiO_2 additives to the samples made them to possess very low oxidation indices .This also resulted in improvement in the bulk densities and cold crushing strength of the sample when compared with those without additives. It was concluded that the addition of SiC/TiO_2 additives improves on the high temperature oxidation resistance of the mullite-carbon ceramic composite sample.
Keywords: titania; kaolin; carbon; sintering temperatures; phases developed; sintered ceramic composite

1. INTRODUCTION

Ceramic materials, which are mostly refractory, are vital for the technological developments being observed today [1, 2]. Imagine how possible it would have being to handle molten metal/alloys before casting into desired components. But the major setback for ceramic materials is their brittleness. This is why the development of refractory ceramic composites to improve on their properties is very important. It has been stated that if monolithic ceramics (unreinforced) is subjected to about 0.1% tensile strain, it will fail catastrophically. But when reinforced with fibers, it could withstand more than 0.5% tensile strain [3-5].

Many researchers have reported their findings on the various work they carried out on ceramic composites. Das and Banerjee, (2000) [6] produced zirconia-mullite composites through solid-state reaction sintering of zircon flour, alumina and dysprosia as sintering additive. Some other researchers [7] employed different processing routes for production of zirconia-mullite composites, which are reaction sintering of alumina and zircon and direct sintering of mullite-zirconia grains by slip casting and sintered at 1600°C for 2 hours. Another group [8] used acicular aluminum borate templates to nucleate textured mullite-zirconia composites prepared from a reactive mixture of alumina and zircon powders. Badiee *et al.* (2001) [9] investigated the effects of CaO, MgO, TiO_2, and ZrO_2 on mullitization of the Iranian andalusite located. They discovered that only zirconia did not encouraged mullite formation from andalusite. Ebadzadeh and Ghasemi (2002) [10] prepared zirconia-mullite composites using α-alumina and aluminium nitrate and zircon powder with TiO_2 as additive. Aramide *et al.* (2014) [11] synthesized mullite-zirconia composites containing yttria as additive. Chandra *et al.* (2013) [12] prepared zirconia-toughened ceramics with a mullite matrix based on the quaternary system ZrO_2-Al_2O_3-SiO_2-TiO_2 in the temperature range 1450-1550°C using zircon-alumina-titania mixtures. Aksel and Komiczny (2001) [13] studied the influence of zircon on the mechanical properties and thermal shock behavior of slip-cast alumina-mullite refractories.

The presence of various additives in the ceramic composite bodies has a lot of influence on the various properties of the ceramic material. Some of these additives aid the formation of the reinforcing component. Different authors have demonstrated that mullitization can be increased by catalytic ions such as Fe^{3+} and Ti^{4+} [14, 15]. These metallic ions help in mullite formation by replacing the Al^{3+} ions in the glass structure during firing. The presence of small amounts of Fe^{3+} and Ti^{4+} in kaolin modifies the chemical composition of the ceramic

bodies and therefore the sintering behavior which in the case of porcelain is characterized by mullitization. Aramide *et al.* (2016) [16] had synthesized mullite-carbon composite from the same materials without any additive. The objective of the present work is to improve the properties of the mullite-carbon ceramic composite through the use of combined titania and silicon carbide.

2. MATERIALS AND METHODS
⌗ Raw Materials
Clay sample used for this study (as mine Kaolin sample) was sourced from Okpella, Edo State southern part of Nigeria, Graphite and titania (TiO_2) were sourced from (Pascal Chemicals, Akure), this were used to maintain the granulometry of the mixture.

⌗ Method
— Processing of raw materials (Graphite and Kaolin)
The raw materials (Spent graphite electrode and kaolin) were crushed into a coarse particle size, of about 10 mm for graphite and less than 2mm for kaolin; the crushed samples were further reduced by grinding using Herzog rod mill. The powdered samples were sieved using 600μm sizes aperture according to ASTM standards in an electric sieve shaker. The undersize that passed through the 600μm sieve aperture were used in the samples making.

— Phase and Mineralogical Composition of Raw kaolin and Graphite
The kaolin clay and graphite samples were carefully prepared for these analyses by digesting in reagents as described by Nabil and Barbara, (2012) [17]. The mineralogical phases present in the samples were determined using X-ray diffractometry (XRD).

3. EXPERIMENTAL PROCEDURE
⌗ Composition calculation using the Rule of Mixtures Technique
Rule of Mixtures is a method of approach to approximate estimation of composite material properties, based on an assumption that a composite property is the volume weighed average of the phases (matrix and dispersed phase). According to Rule of Mixtures [18] the density of composite materials are estimated as follows:

$$\rho_{mixture} = W_{tf\,kaolin} \times \rho_{kaolin} + W_{tf.graphite} \times \rho_{graphite} \qquad (1)$$

$$M_{mixture} = \rho_{mixture} \times vol._{mould}. \qquad (2)$$

where: $\rho_{mixture}$ represent density of the mixture, $M_{mixture}$ is the mass of the mixture, $W_{tf.\,kaolin}$ is the weight fraction of kaolin, ρ_{kaolin} is the density of kaolin, $W_{tf.graphite}$ is the weight fraction of graphite, $\rho_{graphite}$ is the density of graphite and vol.$_{mould}$ is volume of mould.

⌗ Composites Production
The raw materials in the samples making were 3:2vol. % of kaolin and graphite respectively with the addition of 5 and 3 (vol.) % silicon carbide and titania respectively. The mixture were blended thoroughly for proper distribution of constituents materials in a ball mill for 3 hours at a speed of 72 rev/min after weighing via electronic weighing balance in accordance with the composition calculation initially prepared [11, 19]. The resulting blended compositions were mixed with 10% water, the amount of kaolin content in each composition, this was in order to enhance the plasticity of the mixture during compaction. The mixed samples were subjected to uniaxial compaction, which was carried out mechanically under pressure. The molded materials were fired at varying temperatures (1300°C, 1400°C and 1500°C). After which the samples were subjected to various test, to examine the phase analysis, evaluate their physical and mechanical properties.

⌗ Testing
— Shrinkage Measurement
The shrinkage properties of the pressed samples were determined by measuring both the green and fired dimensions, using a digital vernier caliper. The thickness and diameters were measured for evaluation and computation of the shrinkage [19].

$$\% \text{ linear shrinkage} = \frac{(Lg - Lf)}{(Lg)} \; x \; 100 \qquad (1)$$

where Lg represent the green length and Lf represent the fired length.

$$\% \text{ volumetric shrinkage} = \frac{(Vg - Vf)}{(Vg)} \; x \; 100 \qquad (2)$$

where Vg represent the green volume and Vf represent the fired Volume

— Apparent porosity
Test samples from each of the ceramic composite samples were dried out for 12 hours at 110°C. The dry weight of each fired sample was taken and recorded as D. Each sample was immersed in water for 6 hours to soak and weighed while being suspended in air. The weight was recorded as W. Finally, the specimen was weighed when

immersed in water [11, 19]. This was recorded as S. The apparent porosity was then calculated from the expression:

$$\% \text{ apparent porosity } = \frac{(W-D)}{(W-S)} \times 100 \tag{3}$$

─ Bulk Density

The test specimens were dried out at 110°C for 12 hours to ensure total water loss. Their dry weights were measured and recorded. They were allowed to cool and then immersed in a beaker of water. Bubbles were observed as the pores in the specimens were filled with water. Their soaked weights were measured and recorded. They were then suspended in a beaker one after the other using a sling and their respective suspended weights were measured and recorded [11, 19]. Bulk densities of the samples were calculated using the formula below:

$$\text{Bulk density } = \frac{D}{(W-S)} \tag{4}$$

where D represents weight of dried specimen, S represents weight of dried specimen suspended in water, and W represents weight of soaked specimen suspended in air.

─ Cold Compression Strength, Modulus of Elasticity and Absorbed Energy

Cold compression strength test is to determine the compression strength to failure of each sample, an indication of its probable performance under load. The standard ceramic samples were dried in an oven at a temperature of 110°C, allowed to cool. The cold compression strength tests were performed on INSTRON 1195 at a fixed crosshead speed of 10mm min^{-1}. Samples were prepared according to ASTM C133-97 (ASTM C133-97, 2003) [11,19] cold crushing strength, modulus of elasticity and absorbed energy of standard and conditioned samples were calculated from the equation:

$$\text{Cold Crushing Strength} = \frac{(\text{Load to fracture})}{(\text{Surface area of sample})} \tag{5}$$

─ Oxidation Resistance

The fired samples after heat-treatment were cut and the diameter of black portion was measured at different locations and the average value was taken. Lower oxidation index indicates the higher oxidation resistance of the sample [20, 21]. Oxidation index is determined by the formula:

$$\text{Oxidation index } = \frac{\text{Area of oxidized zone}}{\text{Total area}} \times 100 \tag{6}$$

4. RESULTS AND DISCUSSION

⊞ Effects of Sintering Temperature on the Phase Development, Mechanical and Properties of Mullite-Carbon Ceramic Composite Samples

The XRD pattern for the sintered ceramic composite samples are presented in Figure 1 to 3 and Table 1, which shows the addition of 5:3 vol.% SiC and TiO$_2$ respectively, represented as sample D. Figure 4 shows the SEM/EDS data of the samples sintered at the various temperatures.

Table 1. XRD Result of Sintered Sample D Ceramic Composite showing the quantity of different phases present.

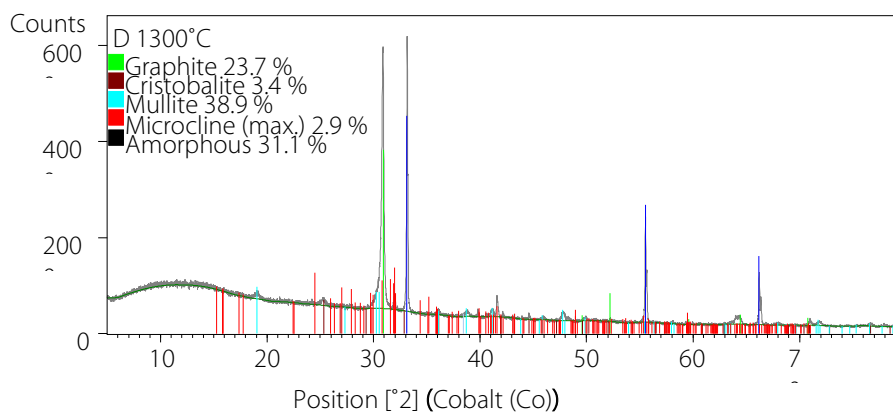| sintered D	Mineralogical/Phase constituent (wt.%)				
Temp. (°C)	Graphite	Cristobalite	Mullite	Microcline	Amorphous
1300	23.7	3.42	38.88	2.94	31.06
1400	18.14	7.67	56.86	1.62	15.71
1500	14.56	8.07	55.57	1.36	20.44

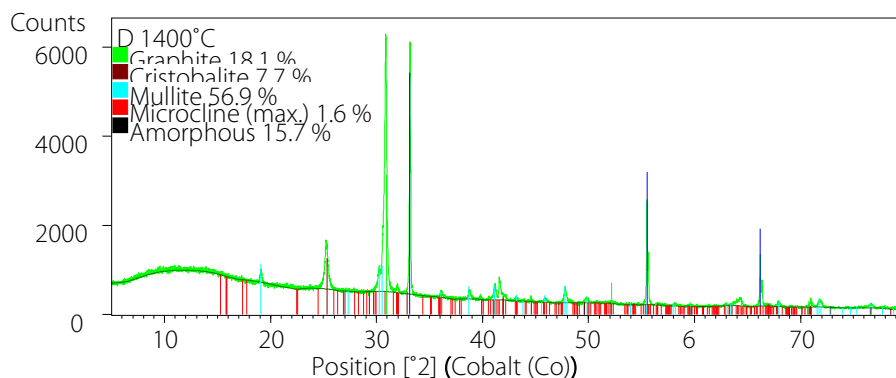Figure 1.X-Ray Diffractometry Pattern of Sample D at 1300°C

Figure 2 X-Ray Diffractometry Pattern of Sample D at 1400°C
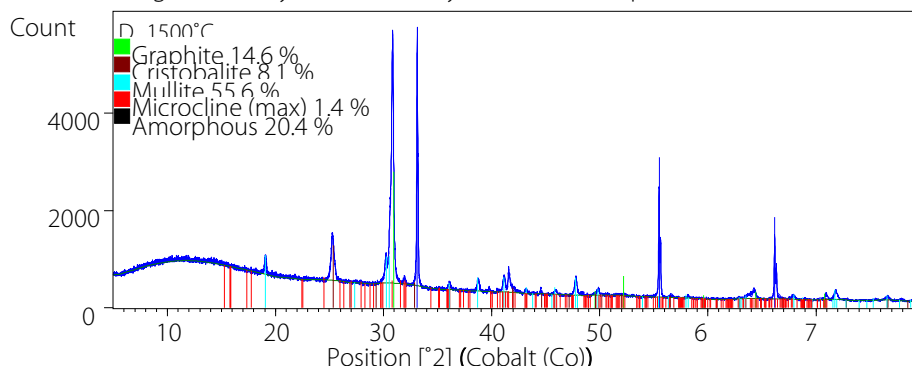

Figure 3.X-Ray Diffractometry Pattern of Sample D at 1500°C
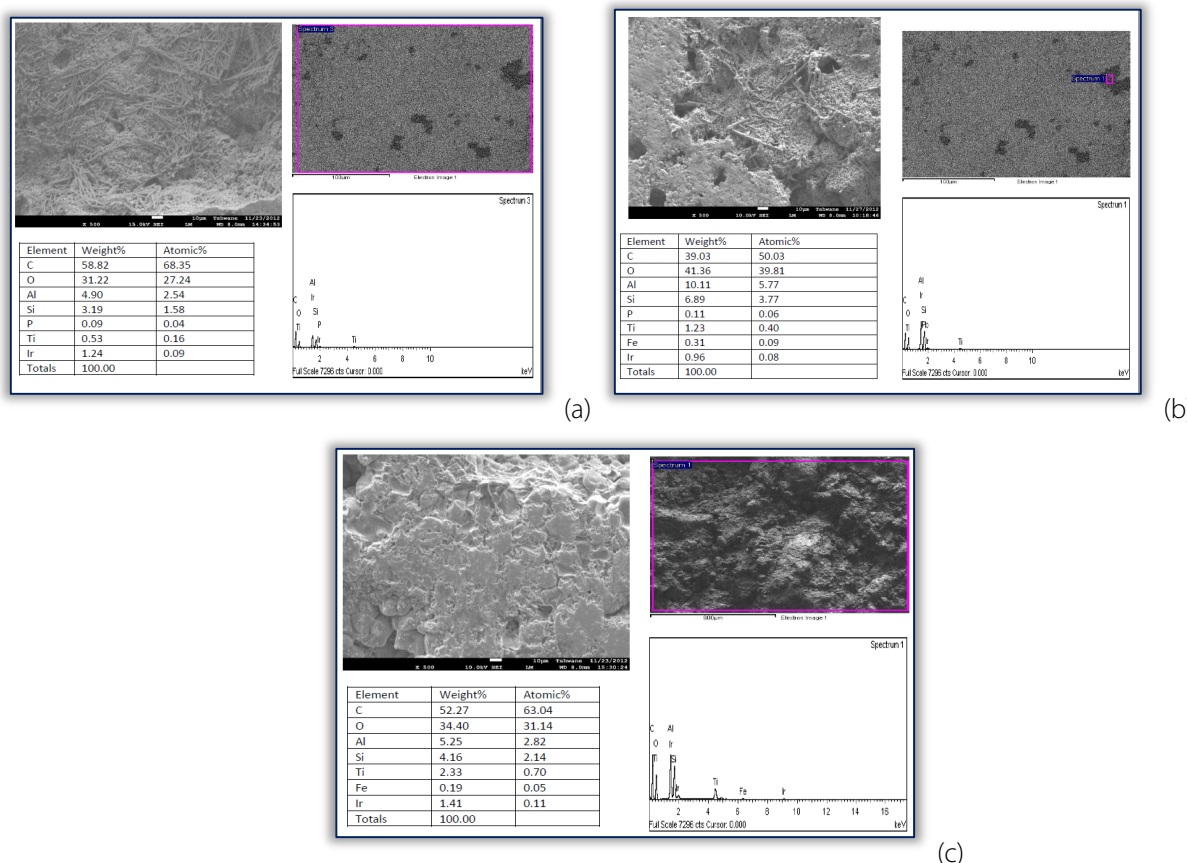

(a)

(b)

(c)

Figure 4. SEM/EDS data of the various samples; (a) Sample D sintered at 1300°C, (b) Sample D sintered at 1400°C and (c) Sample D sintered at 1500°C

From the Table 1, the effects of sintering temperature on the phase development in the sintered ceramic composite samples to which 5 vol.% SiC and 3 vol.% TiO_2 have been added are clearly depicted. From the results obtained from XRD analysis, the sintered sample contains mullite, graphite, amorphous, cristobalite (silica) and microcline phases. It is observed that with an increase in sintering temperature, the mullite phase

increased rapidly from 38.88% at 1300°C to 56.86% at 1400°C. It then reduced slightly to 55.57% when sintered at 1500°C. Similarly, the cristobalite phase is observed to increase from 3.42% at 1300°C to 7.67% as the sintering temperature increased to 1400°C. Further increase in the sintering temperature to 1500°C resulted into cristobalite phase increasing to 8.07%. This is because the kaolinite content of the kaolin undergoes mullitization process as discussed by Aramide et al., (2016) [16].

In the mullitization process, the kaolinite is transformed into mullite and excess silica; this explains the origin of the cristobalite. As observed from the table, the amount of the mullite and cristobalite formed increased generally with the sintering temperature. Moreover, the presence of the titania as an additive in the sample aids the mullitization process. The mullite fibres could be be seen in the SEM images of the samples in Figure 4.

Furthermore, the graphite phase is observed to reduce from 23.7% at 1300°C to 18.14% at 1400°C and then to 14.56% as the sintering temperature is increased to 1500°C. Similarly, microcline is also observed to reduce from 2.94% at 1300°C to 1.62% as the sintering temperature is increased to 1400°C. It further reduced to 1.36% as the sintering temperature is increased to 1500°C. In the case of the microcline (a feldspar mineral) it aids the liquid phase sintering of the ceramic which produce secondary mullite fibers within the ceramic matrix [11]. The explanation for the reduction in the amount of graphite as the sintering temperature increased from 1300°C to 1500°C is that the amounts are measured in percentages, relative to other constituents, once the amounts of cristobalite and mullite increased with increased sintering temperature, it is expected that some other constituents will reduce. Amorphous phase reduced from 1300°C to 1400°C and increased slightly from 1400°C when sintered at 1500°C. Generally, the amorphous content in these sample are more than what was earlier reported [16] for the same sample without any additive.

⌗ Effects of Sintering Temperature on the Physical and Mechanical Properties of the Mullite-Carbon Ceramic Composite Samples

Evaluation of effects of adding 5:3 vol. % SiC/TiO_2 respectively on various physical and mechanical properties of mullite-carbon ceramic composite samples sintered at varied sintering temperature. Below are the results of various physical and mechanical properties of sample D.

— Apparent Porosity

The effect of sintering temperature on the apparent porosity of the ceramic samples is clearly shown in Figure 5 and Table 2. From the Figure, it is observed that the apparent porosity of the sample at 1300°C is 28.571%, as the sintering temperature increase to 1400°C the apparent porosity slightly increased to 29.305% further increase in the sintering temperature to 1500°C leads to an increase in the apparent porosity of the sample to 31.813%. This could be because of

Figure 5. Effects sintering temperature on the apparent porosity of the ceramic sample

the reduction in the amount of graphite contents of the samples as the sintering temperature is increased. The oxidation of some of the graphite in the ceramic sample will leave pores within the matrix of the sample. This could account for the increased porosity as the sintering temperature increased. This implies that the densification reduced with increase in sintering temperature. Some researchers [22-24] have reported that high temperature oxidations of graphite lead to drastic deterioration due to graphite diminution, which result to pores in the samples.
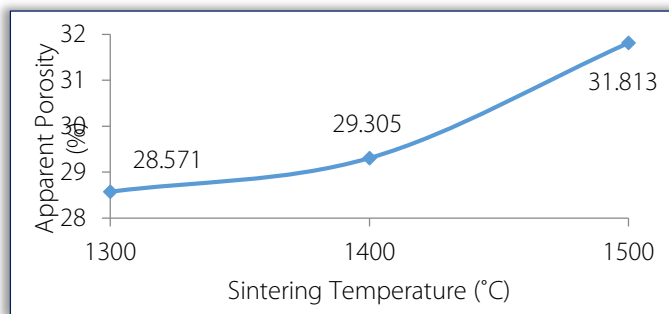
— Bulk Density

The effect of sintering temperature on the bulk density at varied sintering temperature is clearly depicted in Figure 6 and Table 2. From the Figure, it is observed that the bulk density the ceramic sample at 1300°C is 1.75gcm^{-3} as the sintering temperature increased to 1400°C the bulk density increased to its maximum of 2.361gcm^{-3}, further increase in the sintering temperature to 1500°C, the bulk density then reduced to

Figure 6. Effects of sintering temperature on the bulk density of the ceramic sample

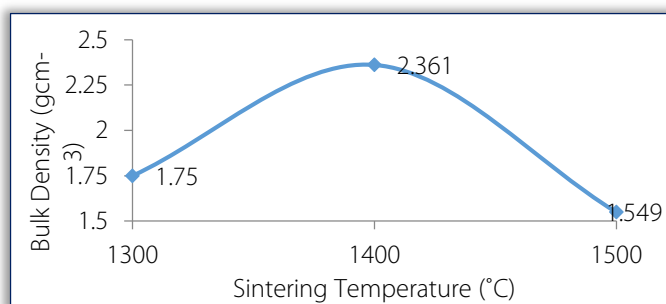1.549gcm^{-3}. It could be stated that the sample attained its maximum densification at 1400°C. Comparing the

above with the results obtained for the samples without any additive [16], it is observed that the bulk densities of the samples were improved upon.

— Cold Crushing Strength

The effect of sintering temperature on the cold crushing strength of the sintered ceramic samples is shown in Figure 7 and Table 2. From the Figure, it is observed that the cold crushing strength of sample at 1300˚C is 8.26 Mpa, 8.22 Mpa at 1400˚C and 6.64Mpa at 1500˚C. This implies that with an increase in the sintering temperature, the cold crushing strength slightly reduced from 1300˚C to 1500˚C. The results correspond to apparent porosity of the sample. The reason for this is that the higher the bulk density of the sample, the higher the load bearing capacity of the sample [2, 25]. It can also be observed cold crushing strength of the samples with SiC/TiO_2, is higher than those without any additive [16].

— Modulus of Elasticity

The effect of sintering temperature on the modulus of elasticity (MOE) of the sintered samples is shown in Figure 8 and Table 2. From the Figure, it is observed that the elastic modulus of the sample at 1300˚C is 14.935Mpa, 14.846Mpa at 1400˚C and 10.114Mpa at 1500˚C. This implies that with an increase in sintering temperature, the modulus of elasticity reduced from 1300˚C to 1500˚C as dictated by the CCS Of the samples. The results correspond to apparent porosity dictation of the sample. The reason for this is that the higher the bulk density of the sample, means that the sample contains more matter to bear the applied load [2, 25].

— Absorbed Energy

The effect of sintering temperature on the absorbed energy of the sintered samples is clearly shown in Figure 9 and Table 2. From the Figure, it is observed that the absorbed energy of sample D at 1300˚C is 6.92 J, 6.82 J at 1400˚C and 5.58J at 1500˚C. This implies that with an increase in sintering temperature, the absorbed energy reduced from 1300˚C to 1500˚C. In this case, the samples followed the CCS variation trend. The results correspond to apparent porosity dictation of the sample. The reason for this is that the higher the bulk density of the sample means that the sample contains more matter to bear the applied load [2, 25].

— Linear Expansion

The effect of adding (5:3) vol. % SiC/TiO_2 respectively on the linear expansion of the sintered samples is clearly shown in Figure 10 and Table 2. From the Figure, it is observed that the linear expansion of sample D is 0.61% at 1300˚C, 1.31% at 1400˚C and 1.8% at 1500˚C. The linear expansion of sample D increased significantly from 1300˚C to 1500˚C.
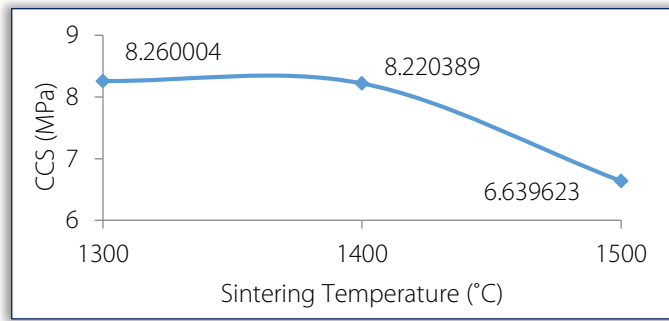

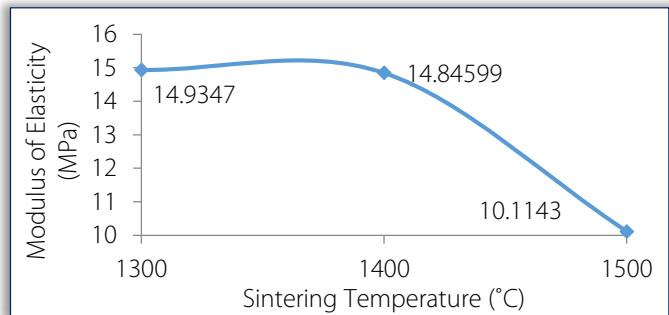Figure 7. Effects of sintering temperature on the cold crushing strength of the ceramic sample

Figure 8. Effects of sintering temperature on the Modulus of Elasticityof the ceramic sample
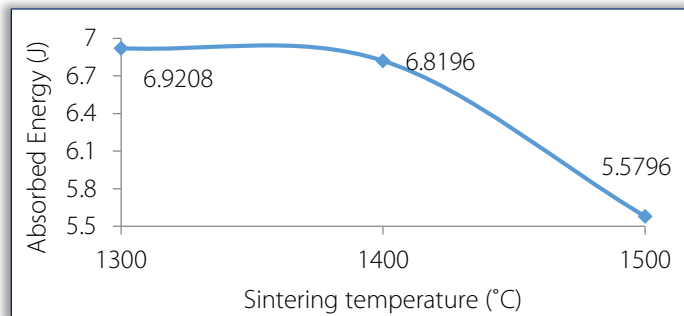

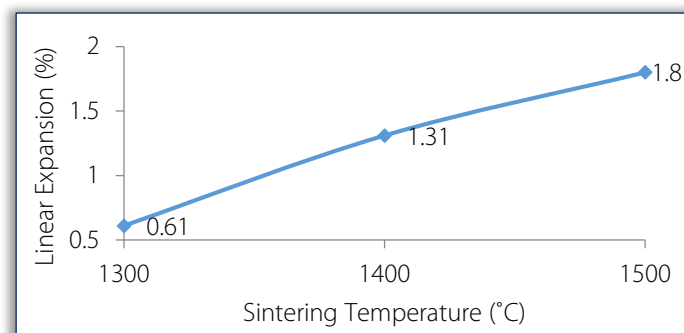Figure 9. Effects of sintering temperature on the Absorbed Energy of the ceramic sample

Figure 10. Effects of Sintering Temperature on the Linear Expansionof Sample D

This implies that an increase in sintering temperature aids the linear expansion of the samples this might be trace to the graphite in the samples. The limited expansion recorded makes the composite to be suitable for high temperature applications. A refractory material should be able to maintain sufficient dimensional stability at high temperatures and after/during repeated thermal cycling [26].

— Volumetric Shrinkage

The effect of adding (5:3) vol. % SiC/TiO$_2$ respectively on the volumetric shrinkage of

Figure 11. Effects of Sintering Temperature on the Volumetric Shrinkage of Sample D

the sintered samples is clearly shown in Figure 11 and Table 2. From the Figure, it is observed that the volumetric shrinkage of sample D is 2.51% at 1300˚C, 2.62% at 1400˚C and 2.9% at 1500˚C. This implies that the volumetric shrinkage of sample D increased slightly from 1300˚C to 1500˚C. This is as achieved for the sample's linear expansion. The limited expansion recorded makes the composite to be suitable for high temperature applications. The volumetric shrinkage of the samples recorded here is smaller than those reported by Aramide et al [16], for the samples without any additive.

Table 2. Summarize the physical and mechanical properties sintered Sample D ceramic composite produced.

Sample D	Physical and Mechanical Properties of the ceramic composite							
Temp. (˚C)	Cold crushing strength (Mpa)	Modulus of Elasticity (Mpa)	Absorbed Energy (%)	Apparent Porosity (%)	Bulk Density (g/cm^3)	Oxidation Index (%)	Linear Expansion (%)	Volumetric Shrinkage (%)
1300	8.26000	14.93470	6.8196	28.571	1.750	0.39	0.610	2.510
1400	8.22039	14.84599	6.9208	29.305	2.361	0.451	1.310	2.621
1500	6.63962	10.11430	5.5796	31.813	1.549	0.635	1.800	2.900

— Oxidation Resistance

The effect of adding (5:3) vol. % SiC/TiO$_2$ respectively on the oxidation resistance of the sintered samples is clearly shown in Figure 12 and Table 2. From the Figure, it is observed that the oxidation index of sample D at 1300˚C is 0.39%, 0.451% at 1400˚Cand 0.635% at 1500˚C. The oxidation index of sample D increased with an increase in sintering temperature from 1300˚C to 1500˚C.

A clear indication that the oxidation resistance reduced as the sintering temerature was increased on adding SiC/TiO$_2$. The SiC present

Figure 12. Effects of Sintering Temperature on the Oxidation Resistanceof Sample D

inhibit oxidation of graphite by reacting with the Oxygen present to form SiO$_2$ that coat the samples from further oxidation of graphite. According to Roy et al. (2014) [27] SiC oxidation in most cases is passive with wide variation in the reaction rates and the morphology of the reaction products.
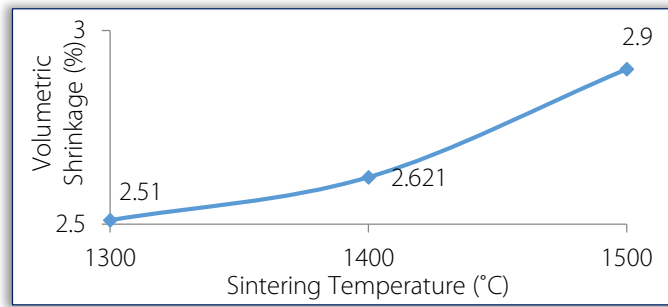

Figure 13. Samples

During passive oxidation, SiO$_2$ liberated forms a dense layer on the surface of SiC which acts as an anti-oxidation protective layer [28]. Studies showed that the layers formed on the composite surfaces acts as physical protection barriers for oxygen penetration. Tripp et al., [29] and Ronald, [30] has reported that reactions where

silica is formed are more desirable for protection against oxidation. Comparing this with the oxidation indices of samples without additives as reported by Aramide *et al* [16], it can be observed that the oxidation indices of the samples with SiC/TiO$_2$ additives are lower than those without any additive. It can be infered that the additves improved on the oxidation resistance of the samples.

Summarily, according to Chester [31], 5 MPa was recommended as the minimum CCS value for refractory clay materials and the acceptable porosity level of refractory is within 10-30 %. This implies that the mullite-carbon ceramic composite developed is suitable for use for high temperature application.

5. CONCLUSIONS

From the data discussed above it is concluded that;

» The addition of SiC/TiO$_2$ additives to the samples made them to possess very low oxidation indices when compared with sample with no additive;
» This also resulted in improvement in the bulk densities and cold crushing strength of the sample when compared with those without additives;
» The addition of SiC/TiO$_2$ additives improves on the high temperature oxidation resistance of the sample
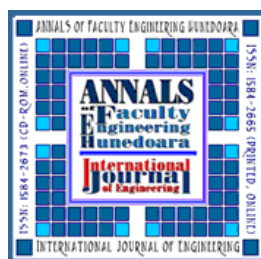
Acknowledgements

Reference

[1] Aramide F.O., Alaneme K.K., Olubambi P.A., Borode J.O., In-Situ synthesis of mullite fibers reinforced Zircon-Zirconia refractory ceramic composite from clay based materials, International Journal of Materials and Chemistry 2015, 5(6), p. 127-139.

[2] Aramide F.O and Seidu S.O. Production of refractory lining for diesel fired rotary furnace from locally sourced kaolin and potter's clay. Journal of Minerals and Materials Characterization and Engineering, 2013; 1: 75 – 79.

[3] Callister W.D., Materials science and engineering: an introduction, 7th ed. John Wiley & Sons, Inc, 2007.

[4] Dag L and Annette M., Advanced Materials and Structures and their Fabrication Processes, Narvik University College, HiN, 2007, p55, 61

[5] Low I.M., Skala R.D., Perera D.S., Fracture properties of layered mullite/zirconia-toughened alumina composites, Journal of Materials Science Letters 13 (1994) 1334-1336.

[6] Das K and Banerjee G. Mechanical properties and microstructures of reaction sintered mullite-zirconia composites in the presence of an additive - dysprosia. Journal of the European Ceramic Society, 2000; 20 (2): 153 – 157.

[7] Rendtorff N.M., Garrido L.B. and Aglietti E.F., Thermal shock behavior of dense mullite–zirconia composites obtained by two processing routes. Ceram. Int. 2008; 34(8): 2017 – 2024.

[8] Ozturk C, and Tur Y.K., Processing and mechanical properties of textured mullite/zirconia composites, J. Eu. Ceram. Soc. 2007; 27, 2-3: 1463-1467.

[9] Badiee H, Ebadzadeh T and Golestani-Fard F. The effect of additives on mullitization of Iranian andalusite, 44th International Colloquium on Refractories, Achen, 126-130, 2001.

[10] Ebadzadeh T., Ghasemi E., Effect of TiO$_2$ addition on the stability of t-ZrO$_2$ in mullite ZrO$_2$ composites prepared from various starting materials, Ceramics International, 2002, 28, p. 447–450.

[11] Aramide F.O., Alaneme K.K., Olubambi P.A. and Borode J.O., Effects of 0.2Y‑9.8ZrO$_2$ addition on the mechanical properties and phase development of sintered ceramic produced from Ipetumodu clay. Faculty Engineering Hunedoara-International Journal of Engineering, 2014; 7(4), 343 – 352.

[12] Chandra D, Das G.C., Sengupta U. and Maitra S., Studies on the reaction sintered zirconia-mullite-alumina composites with titania as additive. Cerâmica, 2013; 59: 487 – 494.

[13] Aksel C and Komicezny F. Mechanical properties and thermal shock behaviour of PSR333 alumina–mullite–zirconia refractory materials. Glass Int., 2001; 1: 16 – 18.

[14] Kausik, D; Sukhen, D. and Swapan, K. D. Effect of substitution of fly ash for quartz in Triaxial kaolin–quartz–feldspar system, J. Eur. Ceram. Soc. 24, (2004), 3169–3175.

[15] Omani, H; Hamidouche, M; Madjoubi, M.A; Louci, K; Bouaouadja, N. and Etude, de la Transformation de trois nuances de kaolin en fonction de la temperature, Silicate Industriel, 65(11–12), 2000, 119–124.

[16] Aramide F.O., Akintunde I.B., Oyetunji A., Insitu synthesis and characterization of mullite-carbon refractory ceramic composite from Okpella kaolin and graphite, Usak University Journal of Material Science, 2016, p. 25-42

[17] Nabil R.B., Barbara Z., Sample preparation for atomic spectrometric analysis: An overview, Advances in Applied science research, 2012, 3 (3), p. 1733-1737

[18] Surappa M.K., Aluminium matrix composites: challenges and opportunities, Sadhana, 28, Parts 1 & 2, 2003, p. 319-334.

[19] Aramide F. O., Effects of sintering temperature on the phase developments and Mechanical properties ifon clay. Leonardo Journal of Sciences 2015; issue 26, p. 67-82.

[20] Kuldeep, Singh (2014): Specially Treated Graphite Fortified Alumina-Silicon Carbide-Carbon Refractories: Fabrication and Properties, Master of Technology Thesis Department of Ceramic Engineering National Institute of technology Rourkela Pp. 17-40.

[21] Subham, M (2013): Expanded graphite fortified magnesia-carbon refractories: fabrication and properties, Master of Technology Thesis Department of Ceramic Engineering National Institute of technology Rourkela Pp. 11-24.

[22] Sadrnezhaad S.K. Nemati Z.A, Mahshid S, Hosseini S and Hashemi B. Effect of Al antioxidant on the rate of oxidation of carbon in MgO–C Refractory, Journal of the American Ceramic Society, 2007; 90 (2): 509 – 515.

[23] Sadrnezhaad SK, Mahshid S, Hashemi B and Nemati ZA., Oxidation Mechanism of C In MgO–C Refractory Bricks, Journal of the American Ceramic Society, 2006; 89(4): 1308 – 1316.

[24] Nemati Z, Sadrnezhaad S and Mooghari HRA., Effect of ferrosilicon, silicon and aluminum antioxidants on microstructure and mechanical properties of magnesia-graphite refractory, Refractories Applications & News, 2005; 10(6): 17-23.

[25] Aramide F.O., Production and characterization of porous insulating fired bricks from ifon clay with varied sawdust admixture, Journal of Minerals and Materials Characterization and Engineering, 2012; 11: 970 - 975.

[26] Gupta O.P., Element of fuels, furnaces and refractories, Romesh Chander Khanna Publishers 2-B, Nath market, Nai Sarak Delhi India Fifth edition, 2010.

[27] Roy J., Chandra S., Das S., Maitra S., Oxidation behaviour of silicon carbide - A review, Rev.Adv.Mater. Sci., 2014, 38, p. 29-39.

[28] Auweter-Kurtz M., Hilfer G., Habiger H., Yamawaki K., Yoshinaka T., Speckmann H.D., Investigation of oxidation protected C/C heat shield material in different plasma wind tunnels, Acta Astronau., 1999, 45, p. 93.

[29] Tripp W.C., Davis H.H., Graham H.C., Effects of SiC additions on the oxidation of ZrB_2, Ceram. Bull. 1973, 52 (8), 612–616.

[30] Ronald A. McCauley, Corrosion of Ceramic and Composite Materials, Marcel Dekker Inc, New York, 2004, 54, 104.

[31] Chester, J.H., Refractories, Production and Properties, The Iron And Steel Institute: London, UK., 1973.